



Published in final edited form as:

J Am Chem Soc. 2020 April 15; 142(15): 6930–6934. doi:10.1021/jacs.0c01722.

Cellular Force Nanoscopy with 50 nm Resolution Based on Integrin Molecular Tension Imaging and Localization.

Yuanchang Zhao¹, Kaushik Pal¹, Ying Tu¹, Xuefeng Wang^{1,2,*}

¹Department of Physics and Astronomy, Iowa State University, Ames, IA 50011, USA

²Molecular, Cellular, and Developmental Biology interdepartmental program, Ames, IA 50011, USA

Abstract

Integrin-transmitted cellular forces have rich spatial dynamics and are vital to many cellular functions. To advance the sensitivity and spatial resolution of cellular force imaging, we developed force-activatable emitter reporting single molecular tension events and the associated cellular force nanoscopy (CFN). Immobilized on a surface, the emitters are initially dark (>99.8% quenching efficiency), providing a low fluorescence background despite the high coating density (>1000/ μm^2) required for sampling cellular force properly. The emitters fluoresce brightly once switched on by integrin tensions and can be switched off by photobleaching, enabling continuous real-time imaging of integrin molecular tensions in live cells. With multiple cycles of molecular tension imaging and localization, CFN reproduces cellular force images with 50 nm resolution. Applied to both migratory cells and stationary cells, CFN revealed ultra-narrow distribution of integrin tensions at the cell leading edge, and showed that force distribution in focal adhesions (FAs) is off-centered and FA size-dependent.

Cellular forces at the cell-matrix interface have been increasingly recognized as important mechanical signals regulating many cellular functions^{1–3} and physiological processes^{4, 5}. Force transmission units such as focal adhesions (FAs) and podosomes have been shown to have ultra-fine structural features^{6–9}, suggesting that cellular forces may have spatial dynamics at nanoscale. Previously, tremendous efforts have been made to visualize cellular force and improve the force imaging resolution. Cell traction force microscopies mapped cellular forces with resolution of microns¹⁰. Lately, surface-immobilized tension sensors convert force to fluorescence, enabling cellular force imaging at diffraction limit^{11–15}. To break the limit, one apparent strategy is to image and localize integrin molecular tensions and reconstruct cellular force maps at ultra-resolution, similarly to the principle of molecular localization adopted in super-resolution light microscopies such as STORM¹⁶ and PALM¹⁷. However, it is highly challenging to image individual integrin tensions at sufficient sampling density with current fluorescent tension sensors. The main difficulty originates from the fact that the tension sensors have non-zero initial fluorescence but have to be densely

*Corresponding Author: xuefeng@iastate.edu.

Supporting Information.

Methods, Supplementary Text, Figures S1–S9, Movies S1–S9

The authors declare no competing financial interest.

immobilized on a surface ($>1000/\mu\text{m}^2$) to probe cellular force at ultra-resolution, causing a high fluorescence background unsuitable for molecular tension imaging.

In this work, we developed a force-activatable emitter which is practically dark but fluoresces brightly once activated by molecular tension (Scheme 1), making it feasible to image and localize integrin molecular tensions with sufficient sampling density. Based on this emitter, we further developed Cellular Force Nanoscopy, termed CFN, for imaging cellular forces with 50 nm resolution. The main construct of a force-activatable emitter is a 18mer DNA/PNA (peptide nucleic acid¹⁸) hybrid duplex labeled with a blackhole quencher 2 (BHQ2), an Arg-Gly-Arg peptide (RGD)¹⁹ as a ligand targeting integrins²⁰, a Cy5 dye, and a biotin for surface immobilization (Scheme 1). The Cy5 is quenched by the BHQ2 until the duplex is forcedly separated by an integrin-RGD-transmitted tension, which de-quenches the Cy5 and switches on the emitter. Compared to the original double-stranded DNA-based tension sensor¹⁵, the DNA/PNA hybrid is resistant to the degradation caused by DNases expressed by cells²¹, and enhances the fluorescence intensity of Cy5 dyes by two-fold (fig. S1) potentially due to protein-induced fluorescence enhancement²². Cy5 instead of Cy3 is used in the emitter because Cy5 is brighter and has shorter lifetime that facilitates emitter switch-off by photobleaching.

During CFN imaging, the emitters are coated at a surface density $>2000/\mu\text{m}^2$ (Fig. 1A, calibrated in fig. S2). On the emitter-coated surface, cells are plated and the integrin molecular tensions constituting cellular forces are continuously imaged by a TIRFM (total internal reflection fluorescence microscope). The initially dark emitters are switched on by local integrin tensions and imaged at the single molecule level. The activated emitters are switched off simply by photobleaching which naturally occurs during imaging and bleaches single Cy5s in 0.5–1 sec. Therefore, force-activatable emitters enable CFN by accomplishing the three standard steps in single molecule localization microscopy: Switch-on, imaging and switch-off (Fig. 1A). By imaging and localizing integrin molecular tensions in many frames, one achieves CFN by superposing tension locations in multiple frames to reconstruct cellular force images with high resolution (Fig 1A, fig. S3).

CFN becomes possible thanks to two previously unrecognized physics effects of a BHQ2-Cy5 pair. First, the BHQ2-Cy5 quenching efficiency in this emitter construct is $>99.8\%$ (calibrated in fig. S4), significantly higher than the previously known values calibrated with ensemble samples²³. The strong quenching leads to low fluorescence background despite the high emitter surface density. Second, we found that a Cy5 near a BHQ2 becomes highly resistant to photobleaching, with its life time extended by 120-fold (Fig. 1B, fig. S5), likely because a BHQ2 absorbs the excitation light for Cy5, not the emission light from Cy5, therefore protecting Cy5 in the non-activated emitters from photobleaching during switch-off process.

We applied CFN to three distinct cell types: anucleate platelets, migratory keratocytes and stationary HeLa cells. In Fig. 1C and Movie S1, a keratocyte produced individual Cy5 fluorescent spots in a good density, showing an optimal switch-on rate. Photobleaching step analysis shows that $>80\%$ fluorescent spots are single Cy5s (fig. S6). The co-imaged F-actin is spatially correlated with Cy5 spots, suggesting that the emitters are likely switched on by

cellular force originating from F-actin. To further confirm that the emitters were activated by integrin tensions, keratocytes were tested on emitters without integrin ligands that showed no emitter switch-on. (fig. S7 and Movie S2).

In Fig. 1D, 100 imaging frames of integrin molecular tensions were continuously acquired in a platelet. By localizing integrin tensions in each frame and superposing 20 frames into one, we obtained CFN images of the platelet (Movie S3). Compared to the rather homogeneous ensemble force image (Fig. 1D), CFN imaging resolved the inhomogeneity in the platelet force map.

We analyzed the precision of tension localization based on an activated emitter in Fig. 1D that was selected and displayed in Fig. 1E. The emitter image shows 11.3 signal-to-noise ratio (SNR) defined as the ratio between the peak fluorescence intensity of a dye in pixels and the standard deviation of the background noise. This leads to $\sigma = 7.3$ nm precision of single molecule localization (refer to supplementary text), and theoretic spatial resolution of $2.35\sigma = 17$ nm for CFN.

Using CFN, we explored the ultra-fine force patterns in lamellipodia and FAs. In Fig. 2, integrin molecular tensions and F-actin dynamics of a migrating keratocyte were co-imaged with 100 frames across 50 seconds in real time (Fig. 2A, Movie S4). Integrin molecular tensions in all frames were localized and superposed to a CFN movie (20 frames per CFN image) (Fig. 2A). In the CFN movie, the force pattern under the lamellipodium consists of two distinct regions, with discrete radial streaks under the cell body, and a smooth and narrow line at the very cell front. Integrin tensions in streaks, colocalized with F-actin, are likely generated by actomyosin which is one of major force sources for integrin tensions²⁴. We speculate that the integrin tensions in the front line are counteracting force supporting actin polymerization that pushes cell boundary forward at the leading edge. To verify above hypothesis, we inhibited actomyosin and actin polymerization with blebbistatin and cytochalasin D, respectively (Fig. 2B, Movies S5 and S6). Inhibiting actomyosin abolished integrin tensions in streaks, but not those in the front line. Oppositely, inhibiting actin polymerization abolished integrin tensions in the front line, but not those in streaks (Fig. 2C). These results suggest that integrins in the cell leading edge are under tension to support local actin polymerization. Their distribution is consistently narrow and can down to 50 nm (shown later in Fig. 4B), suggesting an ultrashort force transmission range from the cell front to local integrins.

Next, we applied CFN to study integrin tensions in FAs. Fig.3A shows a typical process of CFN imaging over FAs, co-imaged with integrin β_3 marking FAs (Movie S7). The integrin tensions were consistently situated within FAs. Compared to the ensemble force images (fig. S8), CFN images of FAs showed that integrin tensions are not homogeneously distributed in FAs. In motile FAs, integrin tensions are preferentially situated at the leading regions of FAs (Fig. 3B and 3C), suggesting that cellular force is off-centered in FAs. We then analyzed the width of force distribution in FAs and found that it generally matches the structural width of FAs if the structural width is above 1 μm . Below 1 μm , however, integrin tensions could cluster in a thin line narrower than the FA width (Fig. 3D–3F), suggesting that FAs have mechanism to concentrate integrin tensions to a much narrower region.

At last, we evaluated the practical spatial resolution of CFN. First, we calibrated the precision of single molecule localization by tracking single surface-immobilized Cy5s across multiple frames and obtained ~16 nm precision σ (Fig. 4A, fig. S9). The spatial resolution of CFN is therefore predicted as $2.35\sigma = 38\text{nm}$. Next, we evaluated the practical spatial resolution of CFN by calibrating ultra-fine force patterns produced by cells. In Movie S8, the keratocyte generated integrin tensions in the front line with a standard deviation $\sigma = 21\text{nm}$ of the tension locations to a fitted curve (Fig. 4B), indicating that the spatial resolution of force imaging is finer than $2.35\sigma = 49\text{nm}$. In HeLa cells, we constantly obtained integrin tensions situated in thin lines in narrow FAs (Movie S9), with 20~30 nm σ to the fitted lines, suggesting that the spatial resolution of CFN reaches 50 nm (Fig. 4C). In addition, we also observed some unique ring-shaped force patterns with a diameter of 200–300 nm out of FAs in HeLa cells (Fig. 4D). These forces may be produced by nascent FAs or endocytosis²⁵. Although the source and mechanism of this type of forces await further investigation, we made use of these force patterns to calibrate the spatial resolution of CFN and obtained values around 50 nm (Fig. 4D).

In summary, we developed low-background force-activatable emitter to image single integrin tensions in live cells in real time. Based on molecular tension localization enabled by this emitter, we developed CFN for cellular force imaging in live cells with 50 nm resolution. CFN has been demonstrated to be a powerful and convenient tool that enables the study of cellular forces at nanoscale in live cells, bridging the resolution gap between cell structural imaging and cellular force imaging, and creating new possibilities for the study of cell mechanobiology.

Supplementary Material

Refer to Web version on PubMed Central for supplementary material.

ACKNOWLEDGMENT

We thank Dr. D. Levine for providing platelet samples. We appreciate the public availability of the single molecule localization code offered by X. Zhuang's group.

Funding Sources

This work was supported by National Institute of General Medical Sciences (1R35GM128747) and National Science Foundation (1825724).

REFERENCES

1. Harburger DS; Calderwood DA, Integrin signalling at a glance. *J Cell Sci* 2009, 122 (2), 159–163. [PubMed: 19118207]
2. Vogel V; Sheetz M, Local force and geometry sensing regulate cell functions. *Nat Rev Mol Cell Biol* 2006, 7 (4), 265–75. [PubMed: 16607289]
3. Wang JH; Thampatty BP, An introductory review of cell mechanobiology. *Biomech Model Mechanobiol* 2006, 5 (1), 1–16. [PubMed: 16489478]
4. Brugues A; Anon E; Conte V; Veldhuis JH; Gupta M; Colombelli J; Munoz JJ; Brodland GW; Ladoux B; Trepas X, Forces driving epithelial wound healing. *Nat Phys* 2014, 10 (9), 683–690. [PubMed: 27340423]

5. Kumar S; Weaver VM, Mechanics, malignancy, and metastasis: the force journey of a tumor cell. *Cancer Metastasis Rev* 2009, 28 (1–2), 113–27. [PubMed: 19153673]
6. Kanchanawong P; Shtengel G; Pasapera AM; Ramko EB; Davidson MW; Hess HF; Waterman CM, Nanoscale architecture of integrin-based cell adhesions. *Nature* 2010, 468 (7323), 580–4. [PubMed: 21107430]
7. van den Dries K; Schwartz SL; Byars J; Meddens MB; Bolomini-Vittori M; Lidke DS; Figdor CG; Lidke KA; Cambi A, Dual-color superresolution microscopy reveals nanoscale organization of mechanosensory podosomes. *Mol Biol Cell* 2013, 24 (13), 2112–23. [PubMed: 23637461]
8. Patla I; Volberg T; Elad N; Hirschfeld-Warneken V; Grashoff C; Fassler R; Spatz JP; Geiger B; Medalia O, Dissecting the molecular architecture of integrin adhesion sites by cryo-electron tomography. *Nat Cell Biol* 2010, 12 (9), 909–15. [PubMed: 20694000]
9. Rossier O; Oceau V; Sibarita JB; Leduc C; Tessier B; Nair D; Gatterdam V; Destaing O; Albiges-Rizo C; Tampe R; Cognet L; Choquet D; Lounis B; Giannone G, Integrins beta1 and beta3 exhibit distinct dynamic nanoscale organizations inside focal adhesions. *Nat Cell Biol* 2012, 14 (10), 1057–67. [PubMed: 23023225]
10. Polacheck WJ; Chen CS, Measuring cell-generated forces: a guide to the available tools. *Nature Methods* 2016, 13 (5), 415–423. [PubMed: 27123817]
11. Morimatsu M; Mekhdjian AH; Adhikari AS; Dunn AR, Molecular Tension Sensors Report Forces Generated by Single Integrin Molecules in Living Cells. *Nano Lett* 2013, 13 (9), 3985–3989. [PubMed: 23859772]
12. Wang X; Ha T, Defining single molecular forces required to activate integrin and notch signaling. *Science* 2013, 340 (6135), 991–4. [PubMed: 23704575]
13. Zhang Y; Ge C; Zhu C; Salaita K, DNA-based digital tension probes reveal integrin forces during early cell adhesion. *Nat Commun* 2014, 5, 5167. [PubMed: 25342432]
14. Blakely BL; Dumelin CE; Trappmann B; McGregor LM; Choi CK; Anthony PC; Duesterberg VK; Baker BM; Block SM; Liu DR; Chen CS, A DNA-based molecular probe for optically reporting cellular traction forces. *Nat Methods* 2014, 11 (12), 1229–32. [PubMed: 25306545]
15. Wang YL; LeVine DN; Gannon M; Zhao YC; Sarkar A; Hoch B; Wang XF, Force-activatable biosensor enables single platelet force mapping directly by fluorescence imaging. *Biosens Bioelectron* 2018, 100, 192–200. [PubMed: 28915383]
16. Rust MJ; Bates M; Zhuang X, Sub-diffraction-limit imaging by stochastic optical reconstruction microscopy (STORM). *Nat Methods* 2006, 3 (10), 793–5. [PubMed: 16896339]
17. Betzig E; Patterson GH; Sougrat R; Lindwasser OW; Olenych S; Bonifacino JS; Davidson MW; Lippincott-Schwartz J; Hess HF, Imaging intracellular fluorescent proteins at nanometer resolution. *Science* 2006, 313 (5793), 1642–1645. [PubMed: 16902090]
18. Nielsen PE; Egholm M; Buchardt O, Peptide nucleic acid (PNA). A DNA mimic with a peptide backbone. *Bioconjug Chem* 1994, 5 (1), 3–7. [PubMed: 8199231]
19. Ruoslahti E, RGD and other recognition sequences for integrins. *Annu Rev Cell Dev Biol* 1996, 12, 697–715. [PubMed: 8970741]
20. Campbell ID; Humphries MJ, Integrin structure, activation, and interactions. *Cold Spring Harb Perspect Biol* 2011, 3 (3), .
21. Dean DA, Peptide nucleic acids: versatile tools for gene therapy strategies. *Adv Drug Deliv Rev* 2000, 44 (2–3), 81–95. [PubMed: 11072107]
22. Hwang H; Myong S, Protein induced fluorescence enhancement (PIFE) for probing protein-nucleic acid interactions. *Chem Soc Rev* 2014, 43 (4), 1221–1229. [PubMed: 24056732]
23. Marras SA; Kramer FR; Tyagi S, Efficiencies of fluorescence resonance energy transfer and contact-mediated quenching in oligonucleotide probes. *Nucleic Acids Res* 2002, 30 (21), e122. [PubMed: 12409481]
24. Murrell M; Oakes PW; Lenz M; Gardel ML, Forcing cells into shape: the mechanics of actomyosin contractility. *Nat Rev Mol Cell Bio* 2015, 16 (8), 486–498. [PubMed: 26130009]
25. Paul NR; Jacquemet G; Caswell PT, Endocytic Trafficking of Integrins in Cell Migration. *Curr Biol* 2015, 25 (22), R1092–105. [PubMed: 26583903]

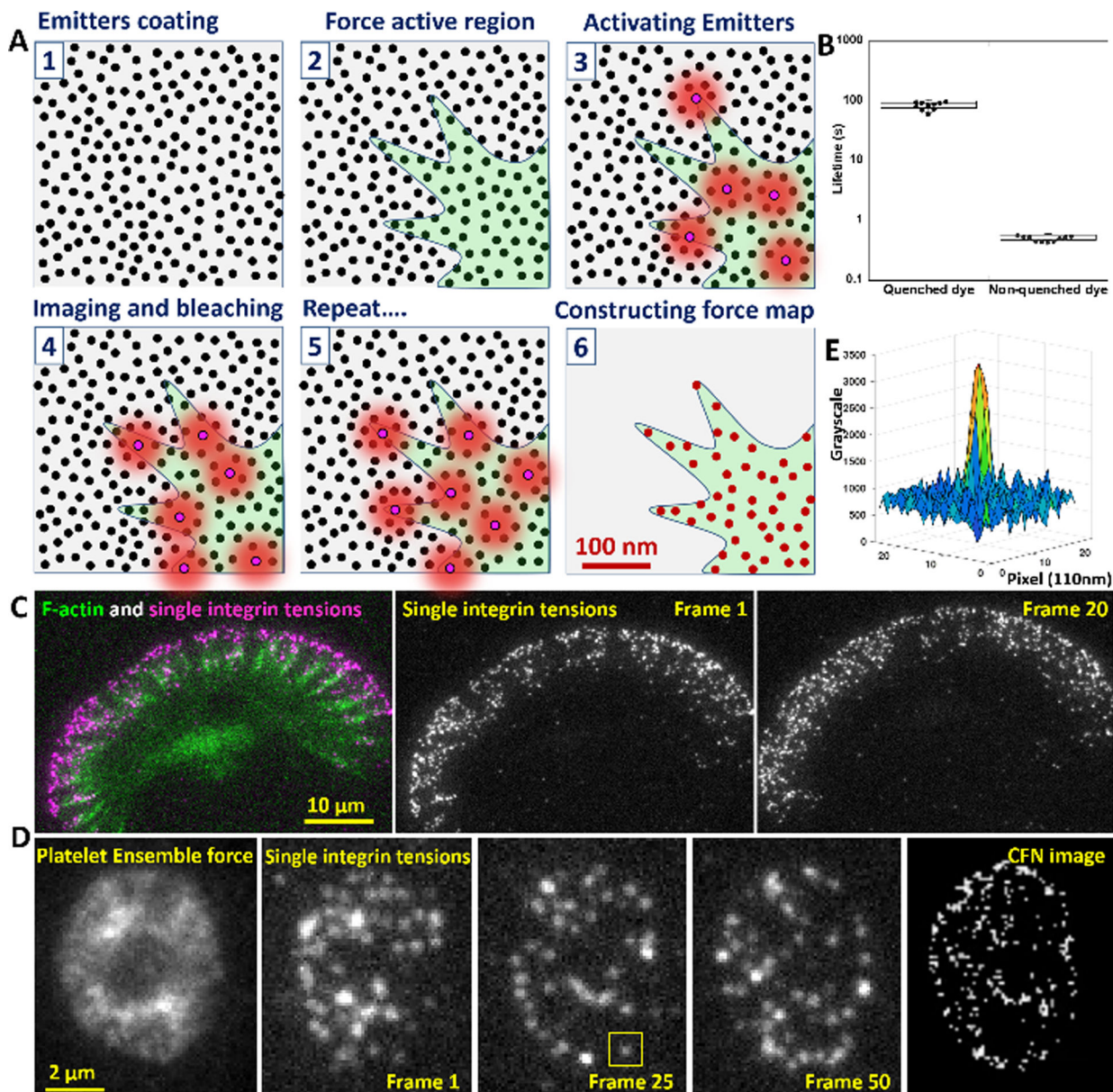


Fig. 1. Principle of CFN and calibration of force-activatable emitter. **(A)** Emitters are coated on a surface at $>2000/\mu\text{m}^2$ (step 1) to provide sufficient sampling density for cellular force (step 2). Emitters are sparsely switched on by local integrin tensions (step 3), imaged by a TIRFM and switched off by photobleaching (step 4). Multiple imaging cycles (step 5) and single molecule localization reconstructs a force map beyond the diffraction limit (Step 6). **(B)** The life time of Cy5 is extended by 120-fold in the proximity of a BHQ2 quencher, so that emitters prior to activation endure the switch-off process by photobleaching. **(C)** Demonstration of time-lapse imaging of integrin molecular tensions in a migrating keratocyte (Movie S1). **(D)** Ensemble force imaging and time-lapse imaging of integrin molecular tensions in a stationary platelet (Movie S3). **(E)** The grayscale map of an activated emitter (yellow squared region in Fig. 1D).

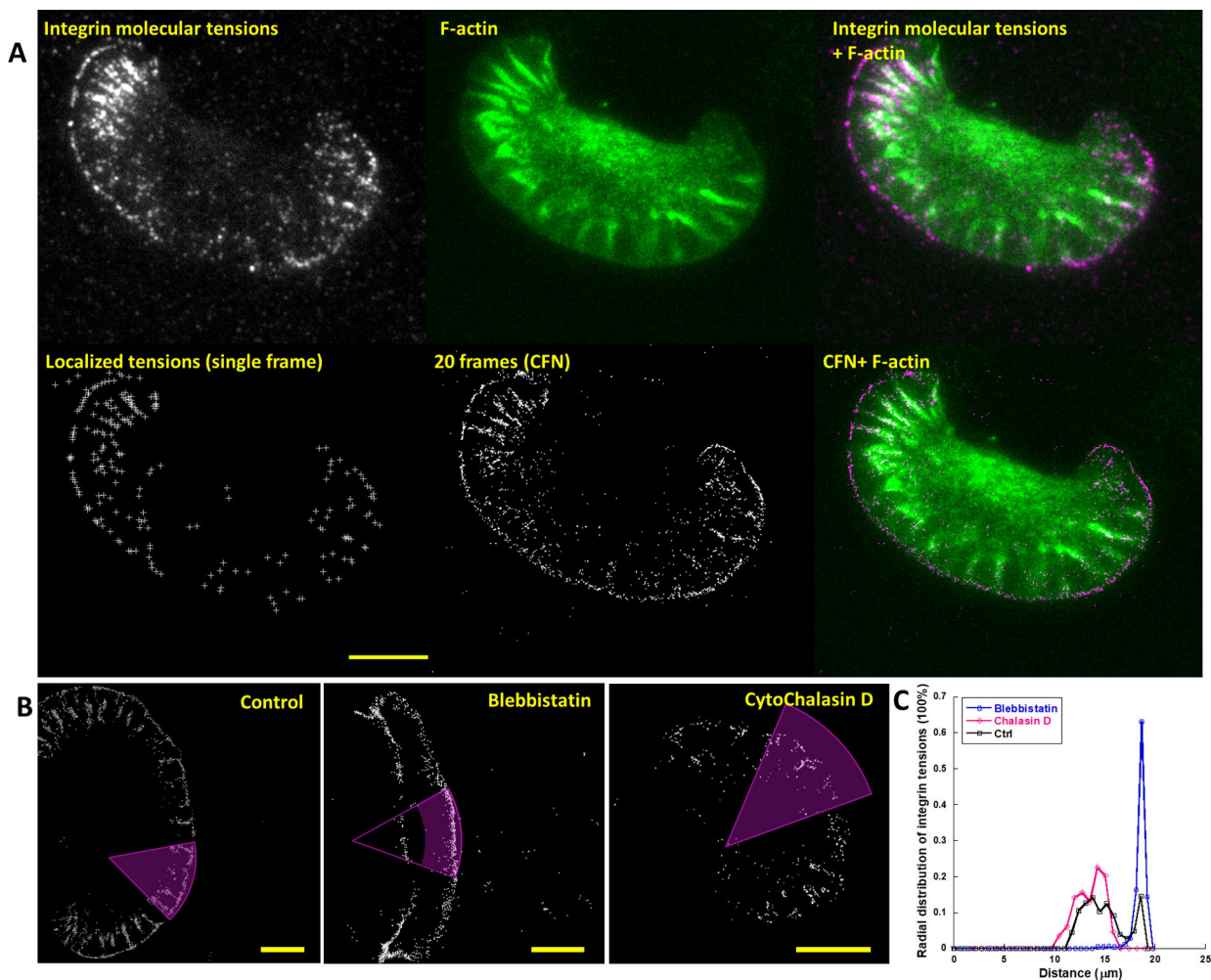


Fig. 2. CFN imaging of integrin tensions under a lamellipodium in migrating keratocytes. **(A)** Single integrin tensions and F-actin were co-imaged (Movie S4). Molecular tensions were localized in each frame (lower left). Every 20 analyzed frames were superposed to a CFN image (lower middle), and merged with F-actin to show the force-structure relation at high resolution. The force pattern consists of a front-line region and streak regions co-localized with F-actin. **(B)** CFN images of keratocytes treated with: DMSO as control (left), 20 μM blebbistatin inhibiting myosin II and cytochalasin D inhibiting actin polymerization (Movies S5–S6). **(C)** Force distribution over the distance to the circular center of the magenta areas. Scale bar: 10 μm .

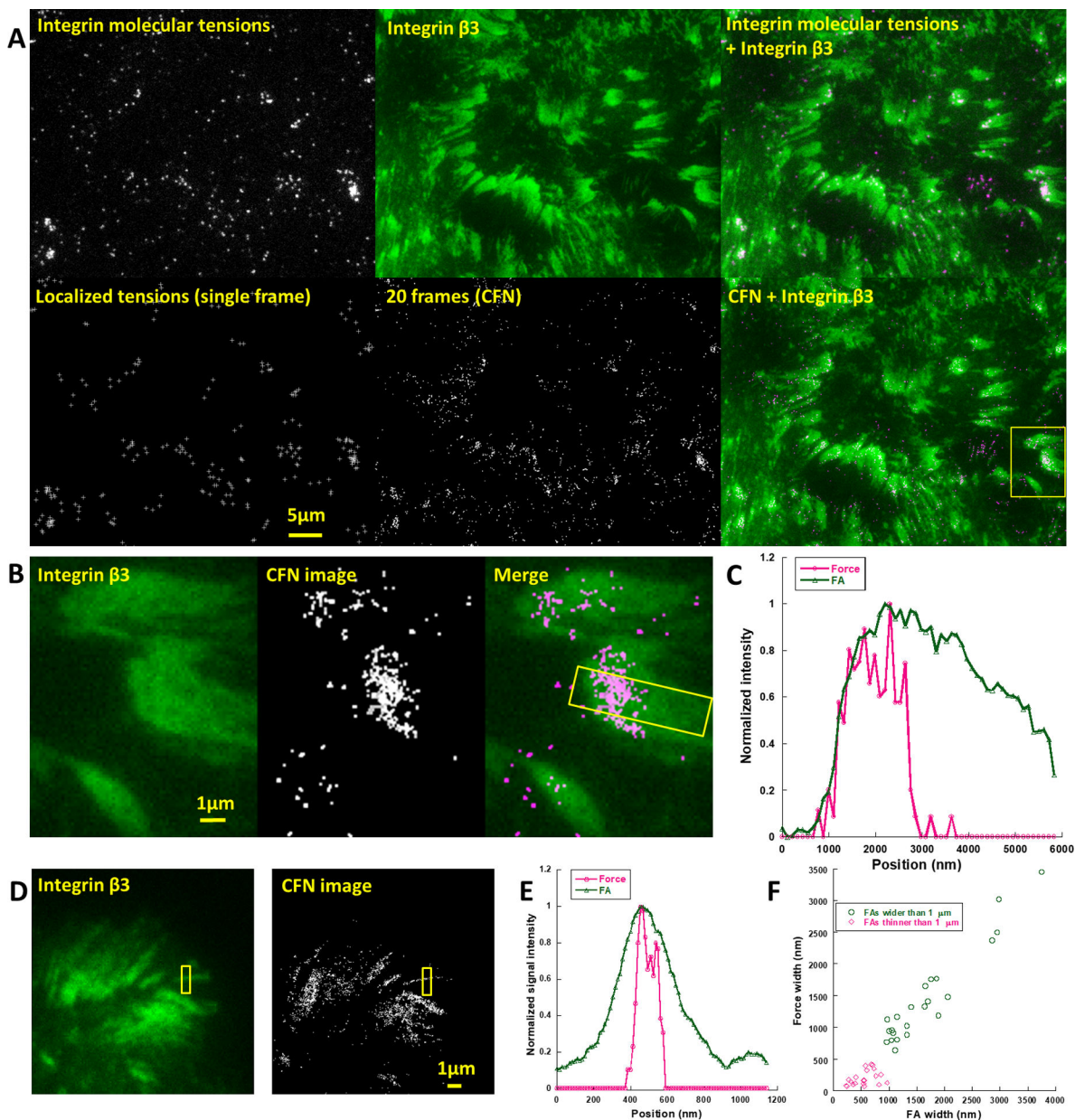


Fig. 3. CFN images of force in focal adhesions. **(A)** Co-imaging of integrin molecular tensions and GFP-fused integrin $\beta 3$ (Movie S7). **(B)** CFN image based on 20 frames (2 min) in a focal adhesion moving towards left. **(C)** Normalized curves of force and integrin distributions in the boxed region in **(B)** along longitudinal direction. **(D)** CFN images based on 100 frames (10 min) in FAs. **(E)** Lateral width analysis of the FA and force distribution in the boxed region in **(D)**. **(F)** The lateral widths of FA and Force distribution in individual FAs.

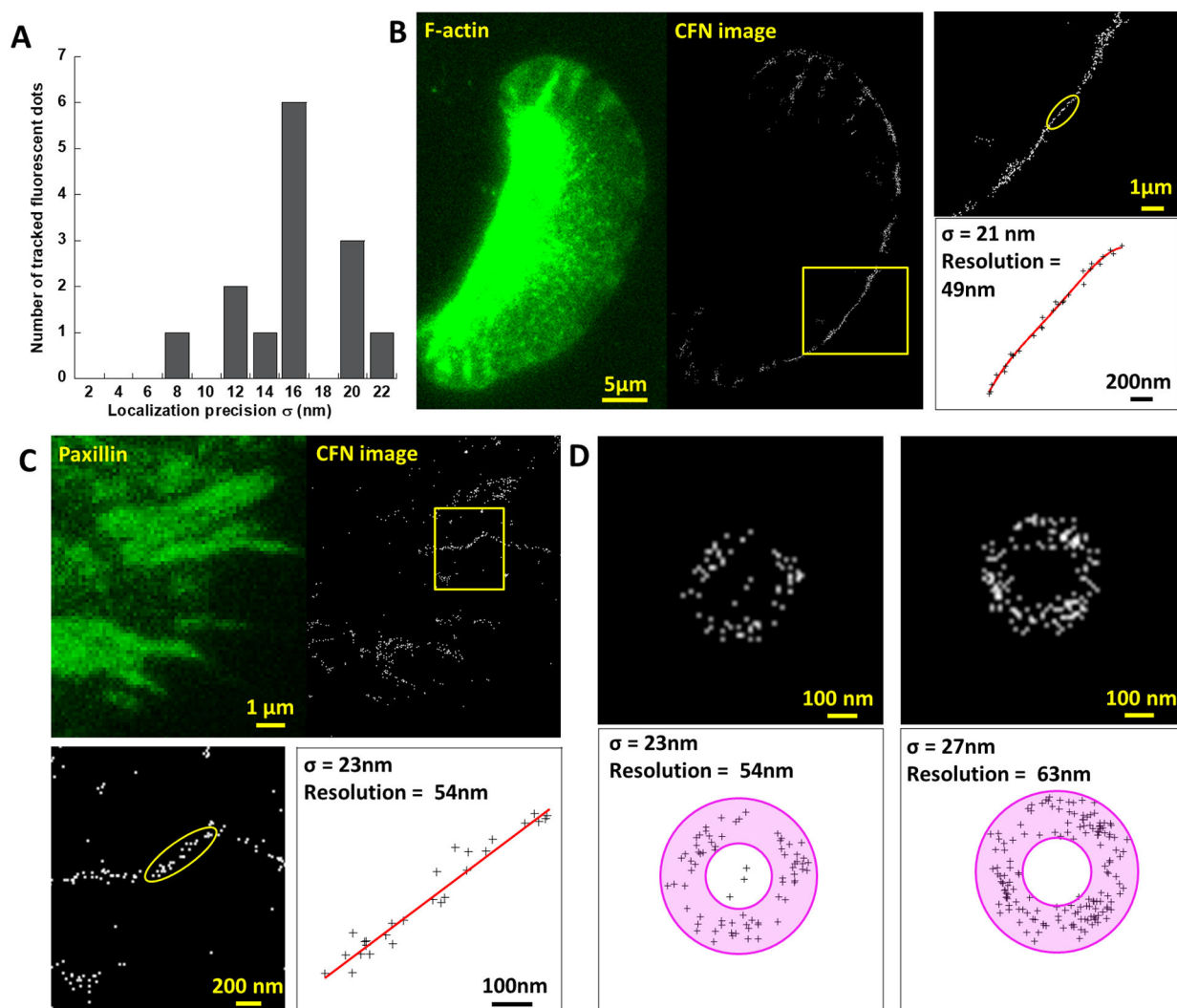
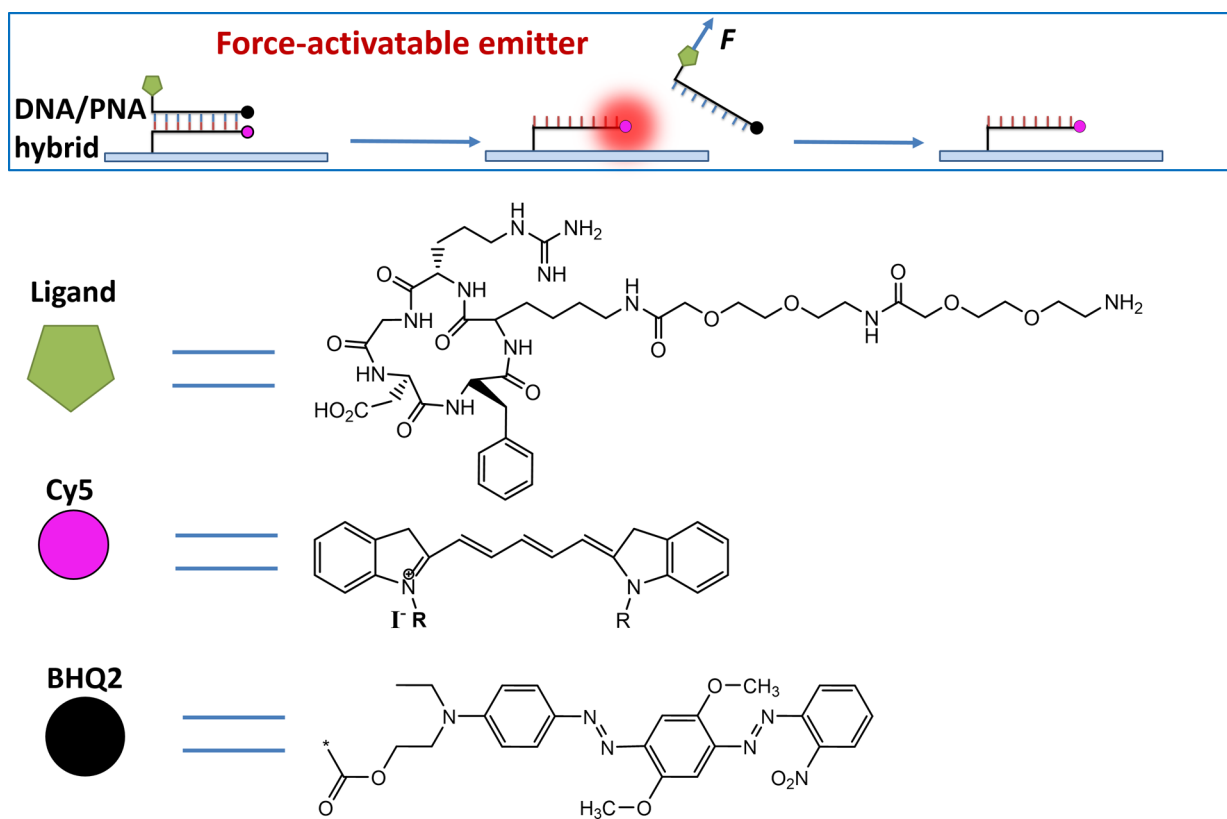


Fig. 4. Calibration of CFN Resolution. **(A)** Single emitter tracking analysis yields 16 ± 4 nm precision in localizing activated emitters. **(B)** 49 nm spatial resolution of CFN was calibrated on the basis of the ultra-narrow force distribution (yellow boxed) in a migration-impeded keratocyte (Movie S8). **(C)** 54 nm resolution of CFN was calibrated on an ultra-thin force pattern in a FA (Movie S9). **(D)** 50–60 nm resolution was calibrated on the basis of integrin tensions in circular patterns. σ was evaluated as the standard deviation of the distances of spots to the circle center.



Scheme 1.
Schematics of force-activatable emitters.